Simultaneous quantitative evaluation of in-plane and out-of-plane deformation by use of a carrier method of large image-shearing shearography

Ping Sun (孙 平)[1], Ruijin Liu (刘瑞金)[2], Qing Han (韩 青)[1], and Xiaofeng Wang (王晓凤)[1]

[1] *College of Physics and Electronics, Shandong Normal University, Ji'nan 250014*

[2] *Department of Mathematics and Physics, Shandong University of Technology, Zibo 255049*

Received April 3, 2006

A carrier method for separating out-of-plane displacement from in-plane components based on large image-shearing shearography is presented. A reference surface is fixed on the side of a test object. They are illuminated by two expanded symmetric illuminations respectively. The carrier is introduced by rotating the reference surface to modulate the displacement of an object. By using Fourier transform to demodulate the modulated fringe pattern, two phase maps, which include out-of-plane and in-plane displacements, can be obtained. Then the out-of-plane displacement can be easily separated from in-plane displacement by subtraction and addition of the two unwrapped phase distributions. The principle of the method is presented and proved by a typical three-point-bending experiment. Experimental results show that the method enjoys high visibility of carrier fringes. The system does not need a special beam as a reference light and has simple optical setup.

OCIS codes: 120.6160, 120.5050, 260.1440.

Shearography[1,2] is a well-established technique for strain measurement and enjoys many favorable characteristics such as its simple optical setup, lower vibration isolation, non-destructive, non-contacting, and direct determination of strain. It has found many applications in non-destructive evaluation[3,4], vibration analysis[5], slope measurement[6], and distance sensing[7], etc.. Therefore, it is a powerful tool for either non-destructive testing of objects under load or for quantitative evaluation of flexural strains. When a large image-shearing Wollaston prism is used in experiment, the out-of-plane deformation or three-dimensional (3D) deformation of an object can be measured by phase-shifting technique, which is known as phase-shifting large image-shearing shearography[8−11]. Large image-shearing shearography can also be applied for deformation by using carrier method[12,13]. Compared with carrier techniques of electronic speckle pattern interferometry (ESPI)[14−16], it enjoys several visible advantages[13]. Because an image of the reference surface is used as reference light, special reference beam is not required. Therefore, it has a simple optical setup. And because the wavefronts scattering from the reference surface and the object are approximatively coaxial, it is less affected by surroundings and has better fringe quality. It does not need to change the optical arrangement to introduce carrier. In this paper, we offer a method for simultaneous quantitative evaluation of in-plane and out-of-plane deformation by using carrier and give attentions to the sensitivity of displacement component. In the optical arrangement presented, the reference surface and the object are illuminated respectively by two object beams, two module 2π phase maps, which include out-of-plane and in-plane displacements, can be obtained with Fourier transform[13]. Then, out-of-plane displacement can be separated from in-plane displacement by easy operation after the two phase maps are unwrapped. The system and some typical experiment results are offered.

The optical arrangement of large image-shearing ESPI system is shown in Fig. 1. A beam from a 40-mW He-Ne laser (633 nm) is divided by a variable beam splitter (VBS) into two illuminating beams, A and B, of equal amplitudes, which lie in x-z plane. A reference object is fixed and adjacent to the test object. Both beams illuminate the object and the reference object symmetrically at angles θ and $-\theta$ with respect to object normal. The scattered light from the object is combined with the reference beam from reference surface through a shearing device and then collected by a charge-coupled device (CCD) camera. The shearing device consists of a Wollaston prism and a polarizer splitting one object point into two in image plane. Thus, the pair of shearing image will be separated from each other if the shearing value of the Wollaston prism is large enough. One image of the object can be superposed on an image of the reference object. The polarizing directions of light from the object and of that from the reference object are perpendicular to each

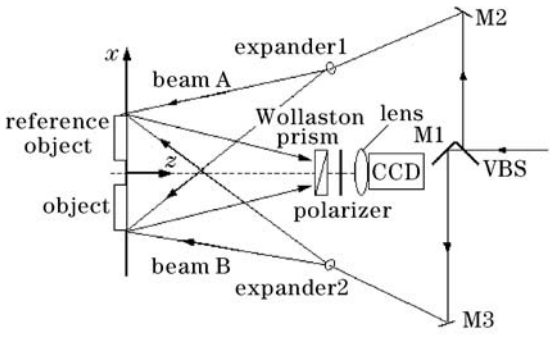

Fig. 1. Schematic of the large image-shearing shearography with dual-beam symmetrical illuminations.

other on image plane. But if the polarization axis of the polarizer orients at an azimuth of 45°, the two superposed speckle images will interfere on image plane. The interference pattern has a higher fringe visibility because scattering light transmitted through the polarizer from the object have nearly the same intensity as the light from the reference object.

At first, the object and the reference object are illuminated by beam A. A speckle pattern before deformation is recorded and stored in computer. Then a series of images are recorded, and subsequently each of them is subtracted from the first one. The subtraction is shown on the monitor. If the reference object is rotated during the operation, carrier fringes are introduced. When the object is loaded, the carrier will be curved due to the modulation of deformation of the object surface. Thus, the spatially modulated fringe distribution can be described by

$$I(x,y) = a(x,y) + b(x,y)\cos\left[\Delta\phi(x,y) + 2\pi f_0 x\right], \quad (1)$$

where $a(x,y)$ and $b(x,y)$ are the unwanted irradiance variations and represent background and modulation terms respectively, f_0 is the carrier frequency introduced by rotation of reference surface, $\Delta\phi$ contains the desired information of deformation of object. By using the carrier and the modulated carrier, $\Delta\phi$ can be derived by Fourier transform[13,17].

When the object is illuminated by two symmetric illuminations, it is essentially two connected interferometers. The interferometer constructed by the combination of the reference surface beam and object beam A is called channel-A interferometer, and the one constructed by the combination of the reference surface beam and object beam B is called channel-B interferometer.

When channel-A and channel-B interferometers are implemented respectively, what we measure is two combinations of in-plane and out-of-plane displacements[1,2]. The phase changes can now be written as[18]

$$\Delta\phi_{\mathrm{A}}(x,y) = \frac{2\pi}{\lambda}[w(1+\cos\theta) + u\sin\theta], \quad (2)$$

$$\Delta\phi_{\mathrm{B}}(x,y) = \frac{2\pi}{\lambda}[w(1+\cos\theta) - u\sin\theta], \quad (3)$$

where w is the out-of-plane displacement of the object along z direction, and u is the displacement component in x direction. The comparison of the phase functions (Eqs. (2) and (3)) by subtraction and by addition gives the pure information of the in-plane displacement and the out-of-plane displacement, i.e.,

$$\Delta\phi_{\mathrm{A}}(x,y) - \Delta\phi_{\mathrm{B}}(x,y) = \frac{4\pi}{\lambda}u\sin\theta, \quad (4)$$

$$\Delta\phi_{\mathrm{A}}(x,y) + \Delta\phi_{\mathrm{B}}(x,y) = \frac{4\pi}{\lambda}w(1+\cos\theta). \quad (5)$$

The experimental setup illustrated in Fig. 1 is employed. The reference object driven by step motor is fixed next to the test object. All of the components are set on a shockproof platform. Two symmetric object beams (A and B) whose wavelengths are 0.6328 μm illuminate the test object at the same incident angle, which is 49.4°, with respect to object normal in x-z plane. The object image area is captured in the normal of the surface with a CCD that has a sensitive area of 768×576 pixels at 8-bit resolution. The CCD sensor receives the reference beam and the scattered light, and, because of the coherent nature of the laser, interference takes place.

The specimen is a cuboid bar made of acrylic glass. It is 150 mm in length, 9.50 mm in width, and 18.50 mm in depth. Young's modulus of the beam is 3.4×10^9 Pa and Poisson ratio is 0.34. The supporting distance is 71.00 mm. The beam's surface is coated with aluminum powder in order to improve its reflection. It is loaded with three points loading and the difference loading is about 75 N.

A 71.0×19.5 (mm) area is measured at a time. The horizontal distance, 71.0 mm, is just the supporting distance in three-point loading. Two object beams illuminate the test object respectively, and the scattered lights interfere with the reference beam on CCD target. The first speckle image of the undeformed object is captured and stored respectively. The object is then deformed after the reference surface is rotated. Two series of images are then captured when beam A and beam B illuminate the object respectively. When the two series of images are subtracted from the first one, fringe patterns can be formed and then phase change maps can be calculated by Fourier transform. Phase unwrapping is necessary to make the phase data continuous because of the phase maps determined modulo 2π[19]. Then the out-of-plane and in-plane displacements can be calculated by using Eqs. (4) and (5).

Figure 2(a) shows the carrier fringe pattern introduced when the object is illuminated by beam A. The carrier bends after loading because of the modulation of the object deformation. Figure 2(b) shows the modulated carrier due to deformation. The wrapped phase map illuminated by beam A can be determined by using Fourier transform, which is shown in Fig. 2(c). Figure 3 describes the carrier fringe pattern introduced (Fig. 3(a)), the modulated carrier (Fig. 3(b)), and the wrapped phase distribution (Fig. 3(c)) corresponding to illumination beam B.

After phase unwrapping, the phase distributions of in-plane displacement component u and out-of-plane displacement component w can be separated from

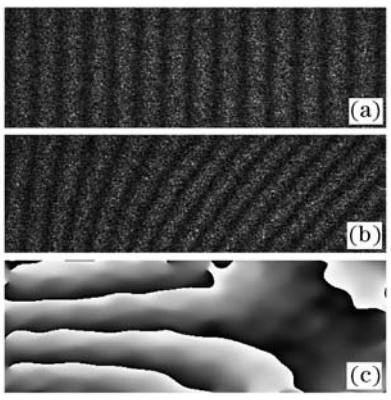

Fig. 2. (a) Carrier fringe pattern before deformation, (b) the modulated carrier fringe pattern after deformation, and (c) wrapped phase map obtained by Fourier transform when beam A is used to illuminate the object.

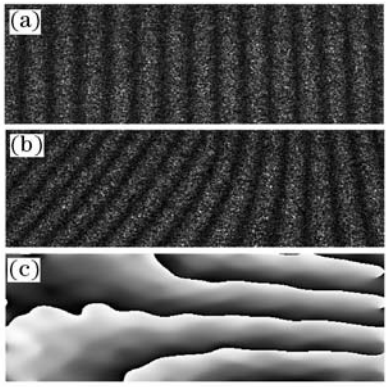

Fig. 3. (a) Carrier fringe pattern before deformation, (b) the modulated carrier fringe pattern after deformation, and (c) wrapped phase map obtained by Fourier transform when beam B is used to illuminate the object.

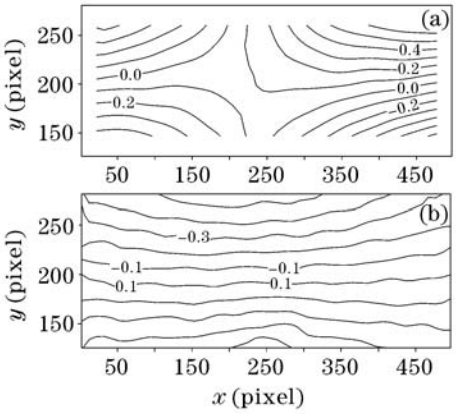

Fig. 4. Contour of in-plane (a) and out-of-plane displacements (b) (unit: μm).

unwrapped phase maps of Figs. 2(c) and 3(c) according to Eqs. (4) and (5). Further calculation is needed to change the phase distribution into quantitative displacement distribution. Figure 4(a) shows the contour of in-plane displacement component in x axis, and Fig. 4(b) shows the contour of out-of-plane displacement component in z axis, where the range of length along x axis is 512 pixels and along y axis is 400 pixels corresponding to 71.0 and 19.5 mm on object surface, respectively.

Using the optical setup of large image-shearing shearography with dual-beam symmetric illuminations and carrier method presented, the out-of-plane displacement and the in-plane displacement can be determined effectively. The presented system enjoys a simple optical setup, high fringe visibility, and an easy way to introduce fringe modulation. Thus this technique would find useful applications in other areas of engineering metrology, particularly in 3D deformation measurement.

P. Sun's e-mail address is sunpingmail@sohu.com.

References

1. R. S. Sirohi, (ed.) *Speckle Metrology* (Marcel Dekker, New York, 1993).
2. P. K. Rastogi, (ed.) *Digital Speckle Pattern Interferometry and Related Techniques* (John Wiley and Sons, Chichester, 2001).
3. Y. Y. Hung, Opt. and Lasers in Eng. **24,** 161 (1996).
4. R. S. Sirohi, C. J. Tay, H. M. Shang, and W. P. Boo, Opt. Eng. **38,** 1582 (1999).
5. L. Yang, W. Steinchen, G. Kupfer, P. Mäckel, and F. Vössing, Opt. and Lasers in Eng. **30,** 199 (1998).
6. Y. M. He, C. J. Tay, and H. M. Shang, Opt. Eng. **38,** 1586 (1999).
7. T. W. Ng, Opt. and Lasers in Eng. **26,** 449 (1997).
8. J. Chen and Y. Hung, Acta Opt. Sin. (in Chinese) **24,** 1292 (2004).
9. P. Sun, H. Wang, X. Zhang, and F. Yang, Acta Opt. Sin. (in Chinese) **23,** 840 (2003).
10. P. Su, X. Zhang, and H. Wang, Chin. J. Lasers B **11,** 189 (2002).
11. Y. Y. Hung, H. M. Shang, and L. Yang, Opt. Eng. **42,** 1197 (2003).
12. H. M. Shang, C. Quan, C. J. Tay, and Y. Y. Hung, Appl. Opt. **39,** 2638 (2000).
13. P. Sun, A. Li, C. Tao, L. Zhang, X. Wang, and Q. Han, Acta Opt. Sin. (in Chinese) **26,** 447 (2006).
14. A. Davila, D. Kerr, and G. H. Kaufmann, Opt. Commun. **123,** 457 (1996).
15. Y. Fu, C. J. Tay, C. Quan, and H. Miao, Appl. Opt. **44,** 959 (2005).
16. P. Sun, C. Tao, L. Zhang, X. Wang, and Q. Han, J. Optoelectronics Laser (in Chinese) **16,** 1093 (2005).
17. M. Takeda, H. Ina, and S. Kobayashi, J. Opt. Soc. Am. **72,** 156 (1982).
18. J. N. Petzing and J. R. Tyrer, J. Strain Analysis **33,** 153 (1998).
19. R. Cusack, J. M. Huntley, and H. T. Goldrein, Appl. Opt. **34,** 781 (1995).